STEM CELLS AND DEVELOPMENT
Volume 00, Number 00, 2014

DOI: 10.1089/scd.2013.0611

ORIGINAL RESEARCH REPORT

Mutation Frequency Dynamics in *HPRT* Locus in Culture-Adapted Human Embryonic Stem Cells and Induced Pluripotent Stem Cells Correspond to Their Differentiated Counterparts

Miriama Krutá,[1,2] Monika Šeneklová,[1] Jan Raška,[1] Anton Salykin,[1] Lenka Zerzánková,[1] Martin Pešl,[1,2] Eva Bártová,[3] Michal Franek,[3] Aneta Baumeisterová,[1] Stanislava Košková,[4] Kai J. Neelsen,[5] Aleš Hampl,[6] Petr Dvořák,[1,2] and Vladimír Rotrekl[1,2]

The genomic destabilization associated with the adaptation of human embryonic stem cells (hESCs) to culture conditions or the reprogramming of induced pluripotent stem cells (iPSCs) increases the risk of tumorigenesis upon the clinical use of these cells and decreases their value as a model for cell biology studies. Base excision repair (BER), a major genomic integrity maintenance mechanism, has been shown to fail during hESC adaptation. Here, we show that the increase in the mutation frequency (MF) caused by the inhibition of BER was similar to that caused by the hESC adaptation process. The increase in MF reflected the failure of DNA maintenance mechanisms and the subsequent increase in MF rather than being due solely to the accumulation of mutants over a prolonged period, as was previously suggested. The increase in the ionizing-radiation-induced MF in adapted hESCs exceeded the induced MF in nonadapted hESCs and differentiated cells. Unlike hESCs, the overall DNA maintenance in iPSCs, which was reflected by the MF, was similar to that in differentiated cells regardless of the time spent in culture and despite the upregulation of several genes responsible for genome maintenance during the reprogramming process. Taken together, our results suggest that the changes in BER activity during the long-term cultivation of hESCs increase the mutagenic burden, whereas neither reprogramming nor long-term propagation in culture changes the MF in iPSCs.

Introduction

Pluripotent stem cells appear to be the source of cells for cell replacement therapy for future generations. The potential use of pluripotent stem cells depends on our ability to expand these cells in vitro for long periods. Unfortunately, human embryonic stem cells (hESCs) undergo adaptation to culture conditions, a process that includes growth acceleration and chromosomal alterations [1–8], some of which resemble tumorigenic events [4,5,9–11]. The reported chromosomal mutations appear to cluster in multiple genes associated with a growth advantage, thus resembling cancer-related mutations in genes such as Bcl2 [8]. These data, together with reports that show increases in loss of heterozygosity (LOH) [12] or copy number variations (CNVs) [13] in late-passage hESCs, demonstrate that the dramatic changes that occur during prolonged cultivation are most likely a consequence of a series of individual mutations [14].

Induced pluripotent stem cells (iPSCs) have also been reported to display an elevated level of mutations. Although a portion of these mutations are inherited from the cells' previous life, whole-genome sequencing of differentiated cells and the corresponding iPSCs showed that 74% of mutations were acquired during reprogramming [15,16]. Nevertheless, an increase in CNVs has been detected in iPSCs [13], and chromosomal aberrations similar to those in adapted hESCs have been identified in iPSCs. Although no dramatic changes have been detected during the ''prolonged'' cultivation of iPSCs [17], no comparable long-term study of hESCs has been published.

[1]Department of Biology, Faculty of Medicine, Masaryk University, Brno, Czech Republic.
[2]International Clinical Research Center, St. Anne's University Hospital Brno, Brno, Czech Republic.
[3]Institute of Biophysics, Academy of Sciences of the Czech Republic, Brno, Czech Republic.
[4]National Tissue Centre, Inc., Brno, Czech Republic.
[5]Novo Nordisk Foundation Center for Protein Research, University of Copenhagen, Copenhagen, Denmark.
[6]Department of Histology and Embryology, Masaryk University, Brno, Czech Republic.

Unfortunately, an increased mutation burden during in vitro cultivation or reprogramming in hESCs and iPSCs, respectively, not only affects the proliferative capacity of the cells but also threatens their terminal use. Changes in hESCs at the genomic level, such as gains of chromosomes 12, 17, and X, resemble germ cell tumors [4,5,10] providing a malignancy model of embryonic carcinoma development [5]. Nevertheless, mutations in certain genes, such as Bcl2, appear to be unique to adapted hESCs [8]. The available data regarding changes in differentiation potential are somewhat contradictory. Some reports have shown a decrease in the ability to differentiate [5,9,10], whereas others have reported no changes in differentiation potential in hESCs with adaptation [18].

Two conceptually distinct approaches are currently used to monitor genomic stability. The first approach analyzes the current state of the genome (using sequencing, LOH or CNV, for example), which is best described by the term ''mutation frequency'' (MF). In contrast, the second approach monitors the mutation rate (MR) in the current culture in which genetic alterations occur, irrespective of the state of the genome at the beginning of the analysis [19]. Although MR determination is connected to laborious population doubling determination that (1) renders the assay more expensive and laborious and (2) the MR can differ based on the calculation method [20,21]. Due to the lack of experimental information regarding the exact number of cell generations required for mutant selection, only the MF is usually reported [21]. To address the degree of genomic instability (represented by the MF), the aforementioned techniques are employed repeatedly to obtain kinetic information. An alternative approach for the quantification of MF dynamics involves reporter gene-based assays. Hypoxanthine phosphoribosyltransferase (*HPRT*) is a readily usable reporter gene, which has been routinely exploited to assess the MF in lymphoblastoid cells [19]. The MF assay is based on screening cells deficient in the *HPRT* gene, which is located on the X chromosome in only one copy per cell. This method, which is based on the selection of mutants, can also be used for MF determination [21]. An *Hprt* reporter mouse was constructed to facilitate the measurement of the MF and MR in mouse embryonic stem cells (mESCs) derived from the reporter mouse [22]. Although the published spontaneous MFs of mESCs vary from 10^{-8} [22] to 10^{-6} [23], these values are still significantly lower than the MFs of differentiated cells (10^{-4}–10^{-5}) [24,25]. Although this model is valuable, it requires a transgenic embryonic stem cell line and is thus not applicable for screening the wide array of available hESC and iPSC lines, particularly for screens of the effects of the activity of DNA repair mechanisms, such as the failure of base excision repair (BER) during hESC adaptation to cultivation conditions or iPSC reprogramming. Thus, we developed an HPRT-based assay that enables the assessment of the MF without prior transgenesis.

Materials and Methods

Cell lines and cultivation

The hESC lines CCTL12, CCTL13, and CCTL14 used in this study were derived in Brno [26]. Passages up to 50 were considered early, whereas passages above 100 (for hESCs) or above 50 (for iPSCs) were considered late passages. Late-passage hESCs exhibited the properties of culture-adapted cell lines reviewed in [27], and an example of their typical characteristics is shown in Supplementary Fig. S1 (Supplementary Data are available online at www.liebertpub.com/scd). Because there is a positive correlation between the signs of adaptation and the length of cultivation, the terms ''late passage'' and ''adapted to culture'' are herein used as synonyms. The iPSC line cl1, obtained from Dr. Majlinda Lako, Institute of Genetic Medicine, Newcastle University (passages 37–80), and the iPSC lines MDMD2Se (passage 28) and AM13 (passage 17), derived in our laboratory from human skin biopsies, were used for iPSC analyses.

hESCs and the iPSC lines cl1 and MDMD2Se were routinely maintained on a feeder layer of mitotically inactivated mouse embryonic fibroblasts (mEFs) and were propagated under previously described cultivation conditions [28], whereas the iPSC line AM13 was maintained under feeder-free conditions using Matrigel hESC-qualified Matrix (BD Biosciences). All the experiments were performed in feeder-free culture using BD Matrigel hESC-qualified Matrix (BD Biosciences) and the mEF-conditioned medium described in detail in [29]. The human foreskin fibroblast (HFF) line SCRC 1042, obtained from the American Type Culture Collection at passages 15–18, and the human ear fibroblast (HEF) line BR 1112203, obtained from the National Tissue Centre at passage 3, were used as differentiated control cells.

Cellular reprogramming

The iPSC lines MDMD2Se and AM13 were created by reprogramming human biopsy cells (adult skin fibroblasts) using the CytoTune™ -iPS Reprogramming Kit (A13780-01; Life Technologies) according to the manufacturer's recommendations, with minor modifications. The iPSC line AM13 was reprogrammed under feeder-free conditions using Matrigel hESC-qualified Matrix (BD Biosciences). The derived iPSC lines were characterized using immunocytochemical staining of pluripotency markers (Supplementary Fig. S2A, B). For the experiments, colonies of iPSCs cultivated on feeder were manually passaged, plated as small clumps on Matrigel (BD) in mEF-conditioned medium supplemented with 20 μM ROCK inhibitor Y27632 (Sigma-Aldrich), and incubated for 24 h after plating. The iPSCs were passaged manually for four passages as colonies; subsequently, they were dissociated to single cells using TrypLE (Life Technologies) and were plated as a monolayer.

HPRT assay

Cells were dissociated using TrypLE and plated (at a density of 1 million cells per one 6-cm Petri dish for pluripotent stem cells or per ten 10-cm Petri dishes for differentiated cells) into a medium containing 6-thioguanine (6-TG; Sigma-Aldrich; 8 μg/mL for the entire course of treatment or 2.5 μg/mL for the first 8 days before changing to 8 μg/mL for pluripotent cells or 7 μg/mL for the entire course of treatment for differentiated cells). When assaying the induced MF, cells were irradiated by ionizing radiation (IR: 0.5 Gy/min; ^{137}Cs; 0.5, 1, or 3 Gy) 24 h after the initial plating. The medium was replaced every 1–2 days during a selection period of 3–4 weeks (5–7 weeks for differentiated cells) until clearly bordered colonies were manually counted. The final MFs were calculated as the ratio of the number of mutant colonies to the plating efficiency of cells in the

nonselective medium at the beginning of the experiment. All the collected data from which MFs were calculated are listed in Supplementary Table S1. Alternatively, cells were incubated in hypoxanthine-aminopterin-thymidine (HAT) medium for 2 days prior to starting the HPRT assay, as previously described [22]. The experiments involving HAT pretreatment and their comparison with HAT-untreated cells are described in detail in Supplementary Table S1.

Inhibition/downregulation of apurinic/apyrimidinic endonuclease

Either methoxamine (MOX; Sigma-Aldrich; 80 μM) or siRNA against apurinic/apyrimidinic endonuclease (APE1) (according to Dvorak et al. [28] and Krutá et al. [30]) was used to inhibit or downregulate APE1. MOX was added to the medium 1 h prior to IR treatment and was left for 24 h. siRNA treatment was performed 48 h prior to the standard HPRT assay.

Immunocytochemical analysis

Immunocytochemical analyses to determine the level of APE1 using rabbit polyclonal anti-APE/Ref1 (Trevigen) and anti-rabbit Alexa 594-conjugated secondary antibody (Invitrogen) were performed as previously described [30]. Rabbit monoclonal anti-Nanog (1:200, 4903S; Cell Signaling) and mouse monoclonal anti-Oct4 (1:250, sc-5279; Santa Cruz Biotechnology) were used. Mouse monoclonal anti-TRA1-81 (1:100) and mouse monoclonal anti-SSEA4 (1:100) antibodies were kindly provided by Peter Andrews, University of Sheffield. The primary antibodies were detected using goat secondary antibodies conjugated to Alexa 594 and Alexa 488 (Invitrogen; 1:500). For H3K27me3 detection, cells were fixed in 4% paraformaldehyde for 10 min at room temperature (RT), permeabilized with 0.2% Triton X-100 for 10 min and with 0.1% saponin (Sigma-Aldrich) for 12 min, and washed twice in phosphate-buffered saline (PBS) for 15 min. Bovine serum albumin (BSA; 1% dissolved in PBS) was used as a blocking solution. Slides with the fixed cells were washed for 15 min in PBS and were incubated with anti-H3K27me3 (Upstate-Millipore; No. 07-449).

Confocal microscopy was performed using a Leica TCS SP5-X system equipped with a white-light laser (wavelengths of 470–670 nm in 1-nm increments), an argon laser (488 nm), ultraviolet lasers (405 and 355 nm), and two hybrid detectors (Leica Microsystems).

Quantitative reverse transcription real-time PCR

Total RNA isolation and quantitative reverse transcription real-time PCR were performed as previously described [29]. The level of Xist was determined using Gene Expression Assays (Applied Biosystems) and normalized to glyceraldehyde-3-phosphate dehydrogenase (GAPDH), and the amplification was performed using a LightCycler 480 II real-time PCR system (Roche).

Flow cytometry analysis

For the cell cycle distribution analysis, a suspension of cells was fixed by 70% ethanol overnight at 4°C. The cells were washed twice in PBS and treated with RNase (Boehringer Ingelheim) at a final concentration of 0.1 mg/mL at 37°C for 30 min. To visualize the DNA, the suspension was incubated with propidium iodide (Sigma-Aldrich; 1 mg/mL) at RT for 15 min. The cell cycle was analyzed using a Beckman Coulter Cytomics™ FC 500 flow cytometer, and the data were analyzed using FlowJo 7.2.2 software. For the detection of the CD30 level, cells in suspension (0.5×10^6) were washed twice in PBS and incubated with an anti-CD30 PE MHCD3004 antibody (Invitrogen; 1:20) in a dilution buffer (0.5% BSA and 2 mM EDTA in PBS) for 15 min at RT. HFF cells were used as a negative control. HL60 cells were used as a positive control [31]. The presence of CD30 was analyzed using a BD FACSCanto II flow cytometer, and the data were analyzed using FlowJo 7.2.2 software.

Cell viability assay

Cells were dissociated to single cells using TrypLE recombinant enzyme (Life Technologies), washed twice with PBS, and counted using a Countess™ automated cell counter (Invitrogen).

Statistical analysis

The data are presented as the mean ± standard error of the mean (SEM). Based on the sampling group, the Mann–Whitney *U*-test was used to evaluate comparisons between two groups. A value of $P \leq 0.05$ was considered significant.

Results

The HPRT assay can be used to evaluate all hESCs, iPSCs, and differentiated cells

Although the HPRT assay has been employed in various cell types, the metabolic nature of selection in 6-TG presents a risk of false-positive and false-negative results when comparing different cell types, such as hESCs, iPSCs, and differentiated cells. Each cell type required a different time for selection and a different concentration of 6-TG. The effective 6-TG concentration was determined as the highest concentration allowing the survival of mutants (Fig. 1A).

To determine whether the concentration of 6-TG affected the outcome of the HPRT assay, either due to incomplete selection at low concentrations or due to excessive killing at high concentrations, the assay was performed with two different 6-TG concentrations. The MF of cells cultivated for the entire period in a medium with a constant 6-TG concentration of 8 μg/mL was compared with the MF of cells treated for 8 days with 2.5 μg/mL 6-TG, followed by 8 μg/mL of 6-TG selection. Spontaneous and IR-induced MFs did not significantly differ at low and high concentrations, suggesting that the concentration of 6-TG in the analyzed range did not affect the outcome of the HPRT assay (Fig. 1A, B).

Neither pluripotent cells nor differentiated cell cultures are burdened by preexisting mutants in the HPRT gene, as demonstrated by pretreatment in HAT medium

The outcome of any mutation assay may be affected by preexisting mutants. To minimize the impact of such mutants in the HPRT assay, preexisting mutants were

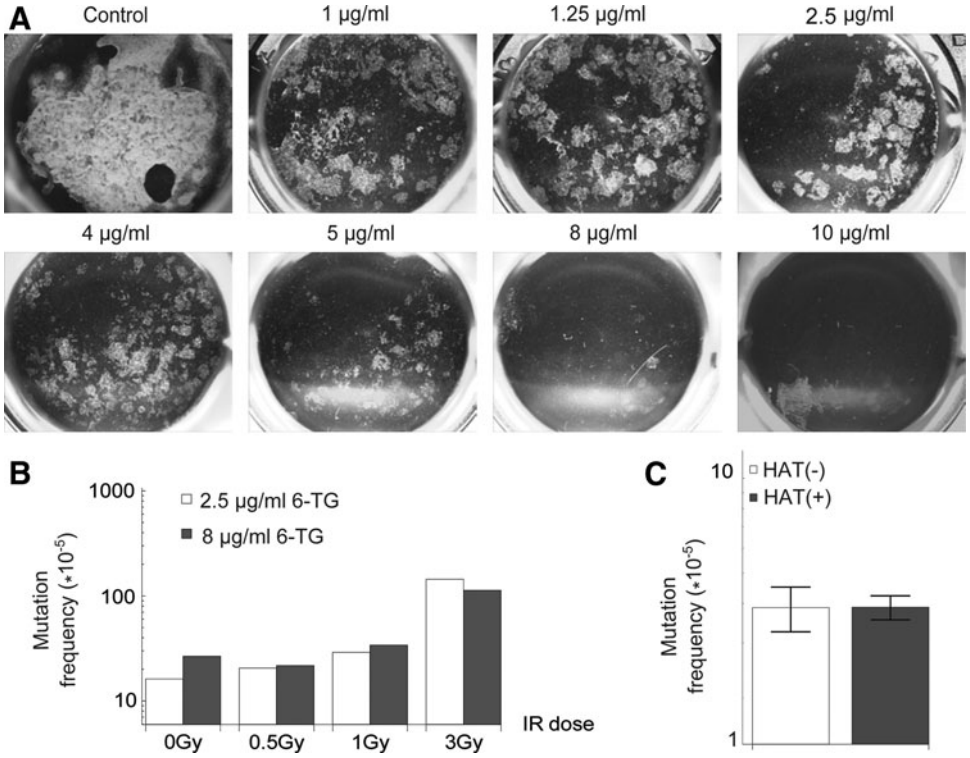

FIG. 1. Neither the concentration of 6-TG nor preexisting mutants in the *HPRT* locus affects the outcome of the HPRT assay. *Panel* **(A)** shows the cytotoxic effect on day 10 of increasing the 6-TG concentration in CCTL14 hESCs, allowing the choice of a suitable concentration for mutant selection. No 6-TG was used in the control sample (Control). *Panel* **(B)** confirms that different concentrations of 6-TG did not affect spontaneous or induced MF upon increasing the dose of IR (IR dose) in hESCs. *Empty bars* show the MF of CCTL14 hESCs cultivated in 8 μg/mL 6-TG throughout entire selection period, whereas *gray bars* show the MF of cells cultivated first for 8 days at a concentration of 2.5 μg/mL of 6-TG and the remainder of the selection period in 8 μg/mL 6-TG. No mutants in the *HPRT* locus accumulated during the previous life of the culture were detected in hESCs; the MF of HAT-pretreated CCTL12 hESCs **(C;** HAT+, *gray bar***)** did not differ significantly from the MF of cells without HAT pretreatment (HAT−, *empty bar*). Error bars represent the mean values and standard errors of three biological replicates. 6-TG, 6-thioguanine; HAT, hypoxanthine-aminopterin-thymidine; hESCs, human embryonic stem cells; HPRT, hypoxanthine phosphoribosyltransferase; IR, ionizing radiation; MF, mutation frequency.

eliminated by cultivation in a medium containing HAT. The combination of these chemicals reliably kills all clones carrying an inactivating mutation in the *HPRT* gene [32].

The preselection of hESC lines in a HAT-containing medium prior to the HPRT assay did not significantly alter the MF of hESCs (Fig. 1C), suggesting a low prevalence of HPRT mutants in the population and allowing us to omit the HAT treatment during routine testing. To verify the reliability of 6-TG selection, the toxicity of the HAT medium was tested on mutants selected in a 6-TG selection medium. To avoid the occurrence of suppressor or reverse mutations in the HPRT locus, and thus, the growth of cells with an active HPRT gene, we also treated cells with a combination of HAT and 6-TG medium. No mutant cell growth was observed in HAT the medium or in the HAT and 6-TG combination medium, demonstrating the efficacy of 6-TG selection (Supplementary Fig. S3).

Only a single HPRT allele is active in hESCs upon 6-TG selection

The presence of only a single copy of the *HPRT* gene is essential to obtain reliable mutagenesis data from the HPRT assay. Considering that the *HPRT* gene is located on the X chromosome, the lack of inactivation of one copy of the X chromosome in female hESCs may impair MF determination in these cells. Thus, we had to ensure that the level of X chromosome inactivation in all the tested cell lines was sufficient to leave only a single active copy of the *HPRT* gene. The H3K27 trimethylation pattern showed no Barr body formation, and lower *XIST* mRNA levels were observed in the female CCTL14 and CCTL12 cell lines compared with a female differentiated cell line (Fig. 2B, C). Despite the abovementioned findings, both the H3K27 trimethylation pattern and the *XIST* mRNA level of the female pluripotent stem cells differed significantly from those of the male CCTL13 line and male fibroblasts (Fig. 2B, C). The inactivated X chromosome in all mutants selected in 6-TG is demonstrated by presence of Barr body (data not shown).

The MFs in two female hESC lines (CCTL12 and CCTL14) and in one male hESC line (CCTL13) were compared (Fig. 2A). The MFs of the hESC lines ranged from $1.73 \pm 0.14 \times 10^{-5}$ SEM to $4.01 \pm 0.76 \times 10^{-5}$ SEM, and the induced (3 Gy) MF ranged from $68.53 \pm 16.32 \times 10^{-5}$ SEM to $81.39 \pm 27.32 \times 10^{-5}$ SEM. No significant difference was found

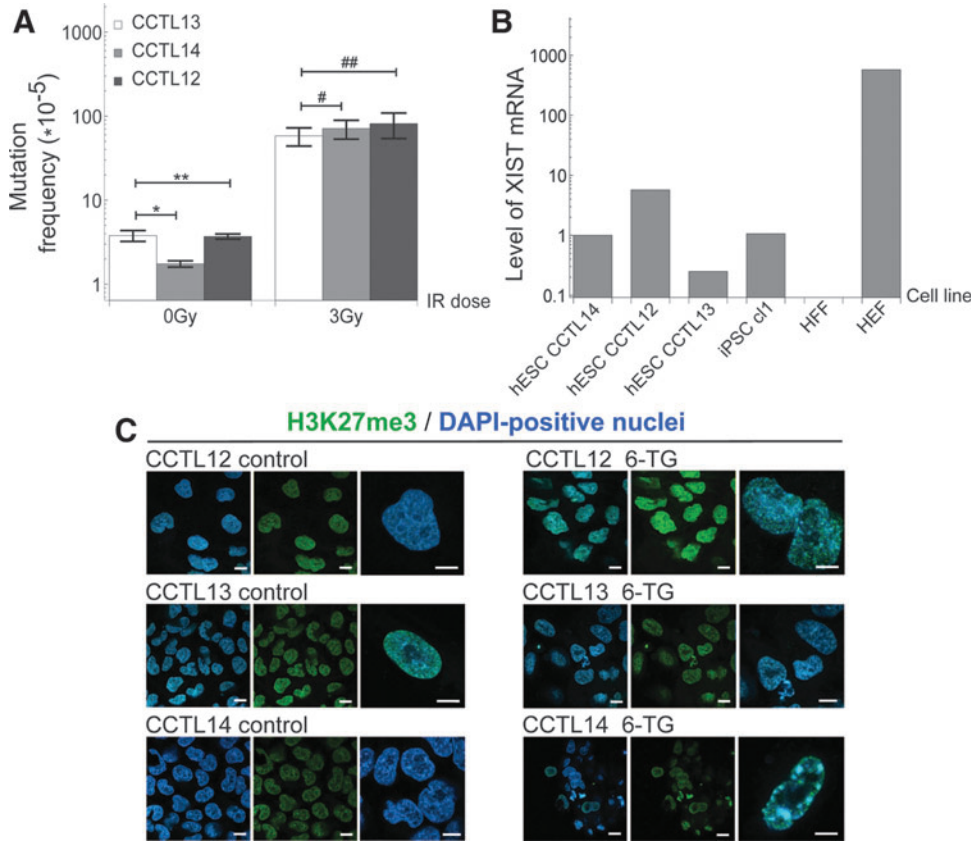

FIG. 2. MF in both male and female hESCs can be measured with the HPRT mutation assay. No significant differences were detected when two female hESC lines (CCTL12 and CCTL14) and one male hESC line (CCTL13) were compared **(A)**. The spontaneous MF of all three hESC lines ranged from $1.73 \pm 0.14 \times 10^{-5}$ to $4.01 \pm 0.76 \times 10^{-5}$, and the induced MF (by 3 Gy IR) ranged from $68.53 \pm 16.32 \times 10^{-5}$ to $81.39 \pm 27.32 \times 10^{-5}$ (the values are the mean ± SEM, $n = 3$; $^{*}P \leq 0.05$, $^{**}P = 0.827$, $^{\#}P = 0.513$, $^{\#\#}P = 0.827$). The Xist mRNA level detected using quantitative reverse transcription real-time PCR was 5- to 30-fold higher in female hESC lines (CCTL14 and CCTL12) compared with a male line (CCTL13; **B**). A female iPSC line (cl1, denoted as iPSC cl1) exhibited a similar Xist mRNA level to female hESCs. Female HEFs and one male HFF were included as controls. No staining of H3K27 trimethylated histones was detected in any tested hESC lines, whereas the characteristic pattern of H3K27 trimethylation was found in the female lines (CCTL12 and CCTL14) after 40 h of 6-TG treatment **(C)**. HEF, human ear fibroblast; HFF, human foreskin fibroblast; iPSCs, induced pluripotent stem cells; SEM, standard error of the mean. Scale bars represent 10 μm.

between the spontaneous and induced MFs either between the two female cell lines or between the CCTL13 (male) and CCTL12 (female; $P = 0.83$) lines. These data show that despite a variable level of inactivation in the tested female hESCs, as indicated by varying trimethylation patterns, the X chromosome inactivation in all the female lines was sufficient for the expression of only a single copy of the *HPRT* gene.

Increased MF is characteristic of culture-adapted hESCs

We measured the characteristics of early and late hESCs to define the groups of nonadapted and adapted hESCs (accelerated proliferation according to Baker et al. [4], cell cycle changes according to Barta et al. [33], and the presence of CD30 according to Harrison et al. and Herszfeld et al. [5,9]). Compared with early passage hESCs, late-passage hESCs grew significantly more rapidly in culture (Supplementary Fig. S2A); accumulated fewer cells in S phase, which corresponds to cell cycle shortening (Supplementary Fig. S2B, C); and exhibited a significantly higher level of CD30 (Supplementary Fig. S2D). These differences indicate an association between the time in culture (passage number) and adaptation to cultivation conditions.

To investigate and analyze genomic instability in culture-adapted hESCs, especially the relation between genomic

TABLE 1. KARYOTYPES OF SELECTED TESTED PASSAGES OF PLURIPOTENT STEM CELL LINES

Line	*Passage range*	*Karyotype*
CCTL12	20–37	46 XX
	102	46 XX, der (7)
CCTL14	20–30	46 XX
	216	47 XX der (12)
	315	47 XX der (12),der (21)
iPSC 11		46 XX der(18)t(2;18)(p13;q23), del(18)(q21).

Karyotyping details are discussed in Lund et al. [27] and Dvorak et al. [28].

iPSCs, induced pluripotent stem cells.

instability and selected chromosomal mutations, we measured MFs in early and late-passage hESCs; the former had normal karyotypes, and the latter corresponded to sublines with either altered or normal karyotypes (Table 1). Our HPRT assay results showed that the long-term cultivation of hESCs was accompanied by the failure of genome maintenance mechanisms; hence, both spontaneous and IR-induced MFs were increased. The spontaneous MF in late-passage CCTL14 hESCs was almost one order of magnitude higher ($16.57 \pm 2.85 \times 10^{-5}$) than the MF of early passage cells ($1.73 \pm 0.14 \times 10^{-5}$; Fig. 3A). Additionally, the induced MF in late-passage cells (IR: 0.5, 1, and 3 Gy; $28.8 \pm 6.28 \times 10^{-5}$, $43.03 \pm 7.79 \times 10^{-5}$, and $260.67 \pm 67.3 \times 10^{-5}$, respectively; Fig. 3A) was significantly higher compared with early passage hESCs ($6.21 \pm 2.44 \times 10^{-5}$, $15.06 \pm 3.62 \times 10^{-5}$, and $77.77 \pm 11.13 \times 10^{-5}$, respectively; Fig. 3A). These results were confirmed in an additional late-passage hESC line (CCTL12) that showed a very similar increase in MF (Fig. 3B).

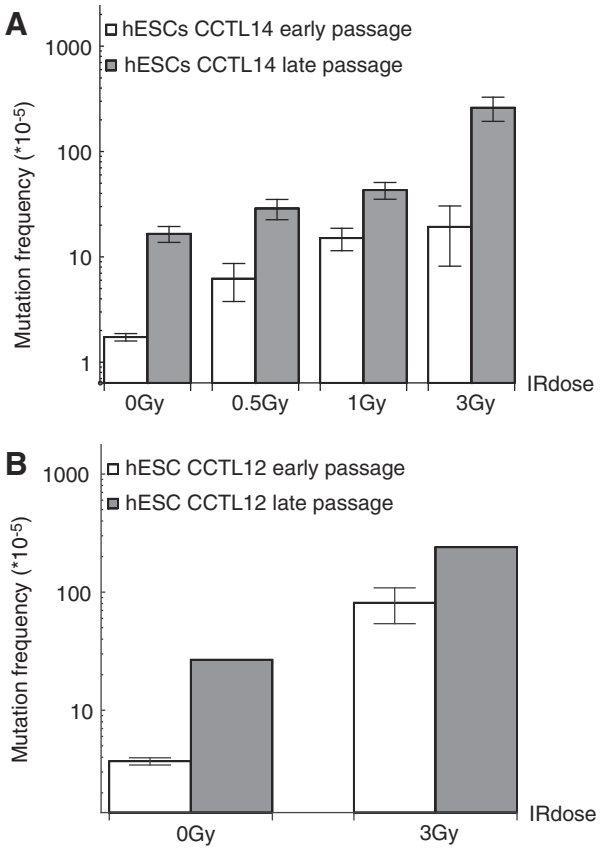

FIG. 3. Spontaneous and IR-induced MFs of hESCs were significantly higher in late passages compared with early passages. The MFs of the CCTL14 **(A)** and CCTL12 **(B)** hESCs were measured after IR treatment (0.5, 1, and 3 Gy), revealing significantly higher spontaneous and induced MFs of late-passage hESCs (*gray bars*) compared with the MF of early passage hESCs (*empty bars*). The MF was calculated as the ratio of mutated colonies formed in a selective medium to the number of mutated colonies formed in a non-selective medium. Error bars (for CCTL14 and early passage CCTL12 only) represent the SEM of at least three biological replicates.

Inhibition or downregulation of APE1 leads to increased MF in hESCs

We previously demonstrated a critical role of reduced BER efficiency in the levels of general and reduced APE1 proteins, particularly in the loss of genomic stability in late-passage hESCs. Based on these data, we used (MOX) to inhibit APE1 function in the CCTL13 cell line to simulate the loss of the APE1 protein, which is associated with the long-term cultivation of hESCs. The inhibition of APE1 activity led to an accumulation of mutations, as demonstrated by the MF increase in MOX-treated cells (Fig. 4). The MOX-treated cells displayed a 1.2- to 2-fold higher spontaneous MF than their untreated counterparts (Fig. 4A). Similarly, the 3 Gy-induced MF of MOX-treated hESCs was

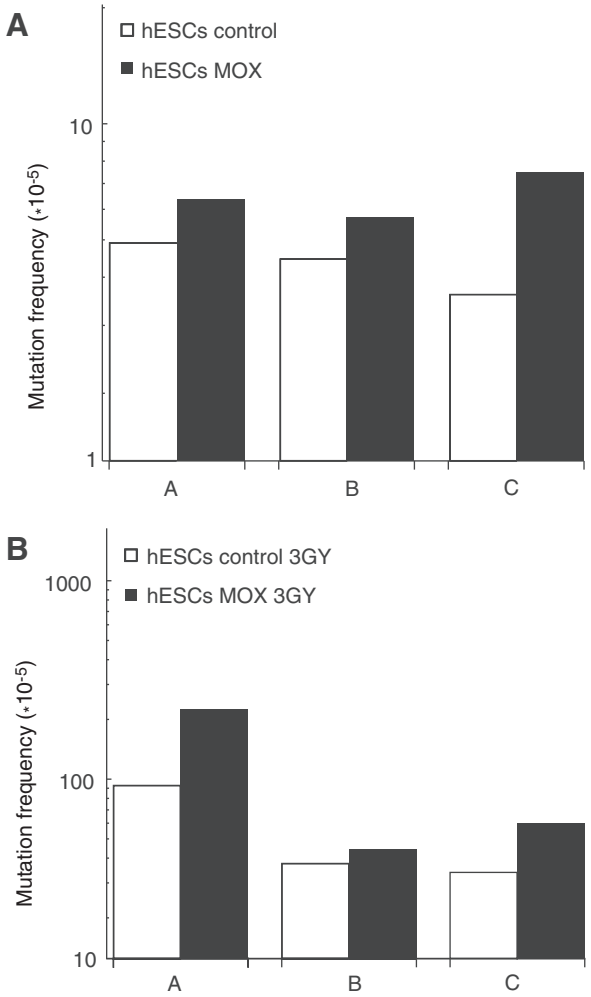

FIG. 4. MOX treatment increases both spontaneous and induced MFs in hESCs. Spontaneous **(A)** and IR-induced (3 Gy; **B)** MFs in three independent biological replicates (A, B, C) of the hESC line CCTL13 were measured using the HPRT assay. The MFs of MOX-treated cells (*black bars*) were compared with the MFs of their untreated counterparts (*empty bars*). The spontaneous and IR-induced MFs of MOX-treated cells were two- to fivefold higher in all the tested replicates compared with untreated cells. MOX, methoxamine.

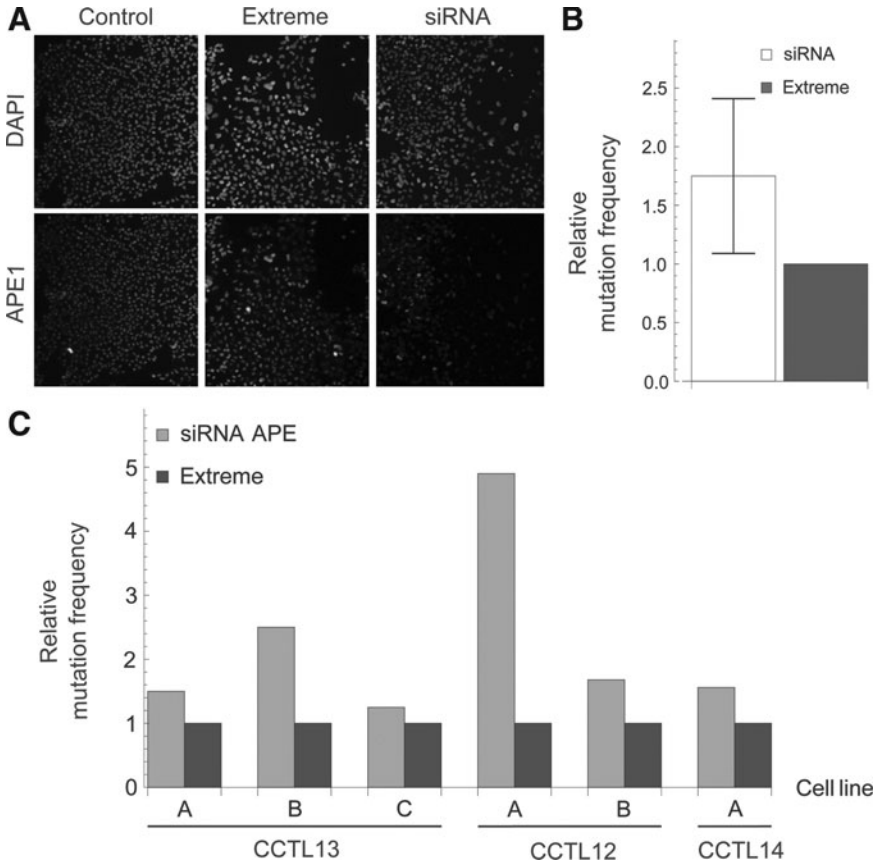

FIG. 5. MF is increased in hESCs with downregulated APE1 expression. hESCs (lines CCTL12, CCTL13, and CCTL14) were treated with siRNA against APE1 to downregulate APE1 expression. The level of APE1 was detected by immunohistochemical analysis (eg, CCTL13; **A**). The level of APE1 in cells treated with siRNA was lower compared with control cells (Control) or cells treated with transfection reagent only (Extreme). Nuclei were stained with DAPI. A statistical analysis of the cells with downregulated APE1 expression (siRNA, *empty bar*; **B**) demonstrated a significantly (1.5×) higher MF relative to mock-treated cells (Extreme, *gray bar*; **B**). The values represent three independent biological replicates. A comparison of the siRNA-induced relative increases in MF among independent biological replicates (A, B, and C) in three cell lines (CCTL12, CCTL13, and CCTL14) is shown (**C**). APE1, apurinic/apyrimidinic endonuclease.

1.2- to 2.5-fold higher than the MF of untreated control cells (Fig. 4B).

Although MOX is considered a specific inhibitor of APE1 [34], we have also developed a model of hESCs with siRNA-mediated depletion of APE1 (Fig. 5A). Consistent with the MOX treatment results, the downregulation of APE1 in the CCTL13 hESC line led to a 1.2- to 2.5-fold increase in spontaneous MF compared with mock-treated cells (Extreme; Fig. 5B). Similar results were obtained with the two other hESC lines, CCTL12 and CCTL14 (Fig. 5C).

MF in iPSCs reaches the level of differentiated cells

Based on published studies, it is well known that iPSCs exhibit higher genomic instability than hESCs (see ''Introduction'' section), although the source of the instability (eg, previous life and reprogramming vs. current mutagenic pressure) remains to be identified. Surprisingly, our data showed similarly high loads (no significant difference) of spontaneous mutations in iPSCs ($14.86 \pm 5.32 \times 10^{-5}$; Fig. 6) and in late-passage ($16.57 \pm 2.85 \times 10^{-5}$) or differentiated cells ($13.94 \pm 1.62 \times 10^{-5}$), whereas the MF values were one order of magnitude lower in early passage hESCs ($1.73 \pm 0.14 \times 10^{-5}$; Fig. 6A).

Even more surprisingly, induction by IR (3 Gy) led to an approximately fourfold higher induction in the MF in late-passage hESCs ($260.66 \pm 67.37 \times 10^{-5}$; Fig. 6A) compared not only with early passage hESCs ($62.2 \pm 9.32 \times 10^{-5}$) but also with iPSCs ($61.8 \pm 15.32 \times 10^{-5}$) and differentiated cells ($77.77 \pm 11.14 \times 10^{-5}$). In contrast to the spontaneous MF, the induced MF of iPSCs did not differ significantly from those of early passage or differentiated cells (Fig. 6A). Multiple iPSC lines were examined using the HPRT assay to determine whether this response is characteristic of iPSCs or is a property of a particular cell line. The spontaneous MF of iPSCs ranged from 7 to 25×10^{-5} (one order of magnitude higher than in early hESCs), whereas IR of 0.5 Gy led to an ~1.3- to 1.5-fold increase, and irradiation with 3 Gy led to a 3.5- to 6.5-fold increase in the MF (Fig. 6B). Despite certain variability among biological replicates, the overall effect of IR on MF was consistent among all the tested cell lines, indicating that the HPRT assay is suitable for assessing mutation pressure in iPSCs.

Discussion

Although the genomic changes at the chromosomal level that are acquired during the process of adaptation to in vitro conditions in hESCs and during reprogramming in iPSCs are well described, the effects of adaptation on the hallmark of genomic stability, that is, the MF, particularly its dynamics, remain unclear. The current methods of assessing genomic stability in hESCs and iPSCs, which are based on CNVs, single nucleotide polymorphisms, and LOH analysis [8,12,14,17,18] and are used to analyze the frequency of mutations/changes, reveal numbers of mutations acquired throughout the previous life of the cell/culture/organism unless analyzed repeatedly. Reporter gene-based assays, in contrast, enable the measurement of not only the sum of preexisting and current mutations but also the actual MR (under special conditions), which refers to mutations acquired during the course of the experiment. To avoid the presence of

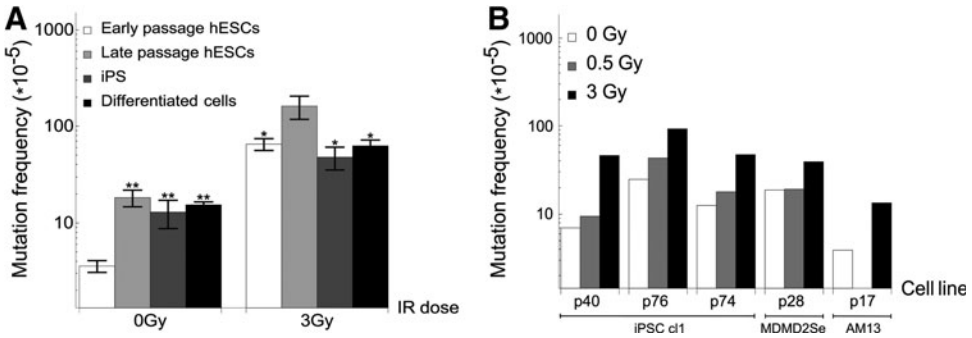

FIG. 6. Similar levels of spontaneous MF in late-passage hESCs and in iPSCs and differentiated cells are significantly higher than in early passage hESCs, whereas late-passage hESCs differ significantly upon induction from all tested cell lines. The MFs of early passage hESCs (Early hESC: *empty bars*), late-passage hESCs (Late passage: *gray bars*), iPSCs (iPSCs: *dark gray bars*), and differentiated cells (Differentiated cells: *black bars*) were compared using the HPRT assay **(A)**. The spontaneous MF of the early passage hESCs was one order of magnitude lower than the MFs of the other analyzed cell lines. The induced (IR: 3 Gy) MF of late-passage hESCs was significantly higher than the MFs of early passage hESCs, differentiated cells, and iPSCs (the values are the mean ± SEM, $n = 3$; $^*P \leq 0.05$ vs. 3 Gy late-passage hESCs). No differences were detected after a prolonged time in culture (cl1, passages p40, p74, and p76 and MDMD2Se, passage p28; **B)** or between different iPSC lines (cl1 and MDMD2Se, **B)**.

preexisting mutants in reporter gene assays based on mutagenesis of the *HPRT* locus, the preselection of hESCs in HAT-containing media can be used to eradicate cells defective in HPRT activity [22]. Therefore, the HPRT assay provides a more accurate assessment of genomic stability in these cells because it reflects the capacity for the maintenance of genomic stability mechanisms in cells, rather than a view of mutations accumulated during the previous life of the cells. However, the distribution of mutants across the whole genome is not uniform [35] and the HPRT assay relies only on the frequency of mutations at the HPRT locus, which biases global mutagenesis data rendering MF data comparable only among other HPRT-based studies. The HPRT assay detected trends between hESCs and iPSCs and between adapted and nonadapted hESCs that were consistent with reports of increase in CNVs in iPSCs [13] and increase in LOH in hESCs [12]. Our results also demonstrated a correlation between an increased MF and karyotypic changes in adapted hESCs.

Although the HAT treatment was effective in suppressing the growth of mutated hESCs (Supplementary Fig. S3), it did not significantly alter the MF measured in the cells investigated in this study (Fig. 1C), suggesting a growth advantage of the unmutated *HPRT* locus in the hESC population, and thus, a low prevalence of HPRT mutants in the hESC population. It is thus possible, under standardized conditions, to omit the HAT-containing medium treatment without affecting the resulting MF.

To date, the use of the HPRT assay has been reported in male mESCs only [22]. The *HPRT* locus is located on the X chromosome, and controversy exists regarding X chromosome inactivation in hESCs [36,37] and iPSCs [38]. It appears that the X chromosome inactivation in hESCs may depend on the cell line, subculture, and passage number [39–42]. The X chromosome has been reported in both the inactive form [43–47] and as two active copies [48,49]. The use of female cell lines with varying levels of X chromosome inactivation might thus affect the HPRT assay results. Our MF data clearly showed that the MFs in both male (CCTL13) and female cell lines (CCTL14 and CCTL12; Fig. 2A) reached the range of 10^{-5}, whereas if both loci were active, the MFs would have to reach a level of 10^{-10}. We thus propose two possible scenarios. Either the level of X chromosome inactivation in hESCs demonstrated by a 5- to 30-fold increase in *XIST* expression in female pluripotent stem cell lines compared with male lines (Fig. 2B) was sufficient to produce only one active copy of the HPRT locus or the X chromosome was inactivated during 6-TG treatment, as demonstrated by its H3K27 trimethylation pattern (Fig. 2C).

The current model suggests a constant rate of *de novo* mutations throughout a prolonged culture period [50]; nevertheless, our data clearly showed a dramatic increase in MF upon prolonged cultivation in vitro (Fig. 3). The increase in MF was also associated with signs of adaptation, such as accelerated growth, cell cycle distribution, and the presence of CD30 (Supplementary Fig. S2). The associations among time in culture, adaptation, and increased MF suggest that adapted cells experience an increased DNA damage rate, decreased checkpoint sensitivity, and/or decreased DNA repair and maintenance activity. Although our study showed no signs of genomic destabilization in late-passage iPSCs, this finding may have been due to the range of tested iPSC passages, which was smaller than that of hESCs. The demonstration of differences in the APE1 locus might shed light on the differences in MFs; however, the available epigenetic data on hESC adaptation are scarce. Nevertheless, Tompkins et al. detected epigenetic changes in genes involved in DNA repair pathways, particularly in BER; they found uracil-N-glycosylase to be differentially regulated in adapted hESCs [51]. Moreover, the dose of reprogramming factors appears to affect CNVs [52], indicating a connection between epigenetics and genomic stability. Data on the differential epigenetic regulation of hESCs and iPSCs are somewhat controversial; the most recent comparison did not find any differences between isogenic hESCs and iPSCs [53,54], whereas others reported abnormalities in iPSC epigenomes [13,14,17,55,56]. Differences could also arise from iPSC epigenetic memory [48,57]. It is thus impossible to form any conclusions regarding the differential epigenetic regulation of the APE1 locus.

The data presented herein answer the question concerning whether the changes in the level of MF are the consequence

of decreases in DNA maintenance associated with long-term cultivation [30] or whether other mechanisms projected to increase MF and the high MF-associated mutations are the reason for the DNA maintenance decrease in hESCs. Considering that similar effects of increases in MF up to 50% were achieved with the inhibition of APE1 in hESCs (MOX or anti-APE1 siRNA; Figs. 5 and 6), it appears rather likely that the increase in MF upon long-term cultivation is at least partially associated with the inhibition of BER activity. Similar effects were observed in iPSCs even as early as ~ 20 passages after reprogramming. The elevated MF in iPSCs corresponds to differentiated counterparts in both the spontaneous and induced MFs, rendering mutation-induced inhibition unlikely and suggesting the presence of a genomic stability maintenance mechanism in iPSCs that has not been reprogrammed, or at least not as efficiently as in hESCs. Surprisingly, despite the equal levels of spontaneous MF in late-passage hESCs, iPSCs, and differentiated cells, both iPSCs and differentiated cells had significantly lower induced MF burdens compared with hESCs. That finding suggests the presence of inducible DNA maintenance mechanisms in iPSCs and differentiated cells, whereas no induction was observed in late-passage hESCs. Further, despite published data to the contrary, the MF in iPSCs was relatively high compared with hESCs, suggesting that mutations are acquired not only during and soon after reprogramming (reviewed in Hussein et al. [58]); instead, the reprogramming most likely did not completely reactivate all the DNA maintenance mechanisms in iPSCs and thus the rate (slope of MF burden) was more rapid in the iPSCs (Fig. 6A) [59].

The MF increase upon BER/APE1 inhibition/down-regulation was somewhat surprising considering that hESCs should possess other mechanisms to prevent such behavior. In a simplistic view, the increase in base damage upon the inhibition of BER should be still safely ameliorated by other means of repair or defense because it has been shown that hESCs possess a functional G1/S checkpoint [60] and elevated levels of mismatch repair [61]), homologous recombination (HR) [62–66], UV sensitivity, coupled nucleotide excision repair [60,67,68], and nonhomologous end joining (NHEJ) [69]). Even if all these mechanisms fail, the combination of replication stress and the subsequent replication collapse caused by an excess of DNA lesions should induce mitotic catastrophe and prevent mutations [70]. We can only hypothesize that either (1) a limited number of lesions was not recognized and did not trigger a replication collapse or (2) error-prone repair mechanisms, such as NHEJ, were employed to eliminate the excess DNA damage. Such a scenario is very likely because it is similar to what occurs in other cell types, such as *Xenopus* oocytes [71]. Moreover, it also has been shown that collapsed replication forks can be repaired by error-prone HR events [72].

Interestingly, BER appears to be important not only for the amelioration of base damage but also to trigger checkpoint control mechanisms by releasing double-stranded breaks as BER-mediated clustered damage repair intermediates [30]. Thus, BER failure not only increases the base damage burden but also renders checkpoints less sensitive.

The discrepancy between the dramatic elevation in the MF in late-passage hESCs and the somewhat mediocre elevation upon APE1 inhibition compared with early passage hESCs (Figs. 3–5) suggests the existence of other mechanisms contributing to genomic instability in late-passage hESCs, such as changes in the activities of HR and NHEJ or in the sensitivity of checkpoints. The absence of a dramatic increase in MF in late-passage iPSCs and the lower level of induced MF in iPSCs, comparable to that in early hESCs (Fig. 6), sustains the hope that such a mechanism can be upregulated in late-passage hESCs, perhaps by the induction of APE1 or another mechanism. Discovering such mechanisms in late-passage hESCs and targeting them by genetic or chemical interventions would enable prolonged cultivation without an increase in MF. Unfortunately, such mechanisms have yet to be discovered.

Acknowledgments

The authors wish to thank Martina Vodinská and Miroslava Nehybová for their technical support, Kamil Matulka from Masaryk University for reading the article, and Duncan Baker from the University of Sheffield for hESC karyotyping. We also thank Majlinda Lako from Newcastle University for the cl1 iPSCs, Stjepan Uldrijan from Masaryk University for the HL-60 cell line, and Peter W. Andrews from the University of Sheffield for the Tra 1-81 and SSEA4 antibodies. This work was supported by grants from the Grant Agency of the Czech Republic (no. GA13-19910S and P302/12/G157); project FNUSA-ICRC (no. CZ.1.05/1.100/02.0123) from the European Regional Development Fund; a grant from the Ministry of Education, Youth and Sport of the Czech Republic (MSM0021622430); and European Commission FP6 funding (contract LSHG-CT-2006-018739) and grant no. CZ.1.07/2.3.00/30.0009 cofinanced by the European Social Fund and the state budget of the Czech Republic.

Author Disclosure Statement

No competing financial interests exist.

References

1. Draper JS, HD Moore, LN Ruban, PJ Gokhale and PW Andrews. (2004). Culture and characterization of human embryonic stem cells. Stem Cells Dev 13:325–336.
2. Imreh MP, K Gertow, J Cedervall, C Unger, K Holmberg, K Szöke, L Csöregh, G Fried, S Dilber, E Blennow and L Ährlund-Richter. (2006). In vitro culture conditions favoring selection of chromosomal abnormalities in human ES cells. J Cell Biochem 99:508–516.
3. Spits C, I Mateizel, M Geens, A Mertzanidou, C Staessen, Y Vandeskelde, J Van der Elst, I Liebaers and K Sermon. (2008). Recurrent chromosomal abnormalities in human embryonic stem cells. Nat Biotechnol 26:1361–1363.
4. Baker DEC, NJ Harrison, E Maltby, K Smith, HD Moore, PJ Shaw, PR Heath, H Holden and PW Andrews. (2007). Adaptation to culture of human embryonic stem cells and oncogenesis in vivo. Nat Biotechnol 25:207–215.
5. Harrison NJ, D Baker and PW Andrews. (2007). Culture adaptation of embryonic stem cells echoes germ cell malignancy. Int J Androl 30:275–281; discussion 281.
6. Lefort N, M Feyeux, C Bas, O Féraud, A Bennaceur-Griscelli, G Tachdjian, M Peschanski and AL Perrier. (2008). Human embryonic stem cells reveal recurrent genomic instability at 20q11.21. Nat Biotechnol 26:1364–1366.

7. Mitalipova MM, RR Rao, DM Hoyer, JA Johnson, LF Meisner, KL Jones, Dalton S and SL Stice. (2005). Preserving the genetic integrity of human embryonic stem cells. Nat Biotechnol 23:19–20.
8. Amps K, PW Andrews, G Anyfantis, L Armstrong, S Avery, H Baharvand, J Baker, D Baker, MB Munoz, et al. (2011). Screening ethnically diverse human embryonic stem cells identifies a chromosome 20 minimal amplicon conferring growth advantage. Nat Biotechnol 29:1132–1144.
9. Herszfeld D, E Wolvetang, E Langton-Bunker, T-L Chung, AA Filipczyk, S Houssami, P Jamshidi, K Koh, AL Laslett, et al. (2006). CD30 is a survival factor and a biomarker for transformed human pluripotent stem cells. Nat Biotechnol 24:351–357.
10. Enver T. (2005). Cellular differentiation hierarchies in normal and culture-adapted human embryonic stem cells. Hum Mol Genet 14:3129–3140.
11. Blum B and N Benvenisty. (2009). The tumorigenicity of diploid and aneuploid human pluripotent stem cells. Cell Cycle Georget Tex 8:3822–3830.
12. Närvä E, R Autio, N Rahkonen, L Kong, N Harrison, D Kitsberg, L Borghese, J Itskovitz-Eldor, O Rasool, et al. (2010). High-resolution DNA analysis of human embryonic stem cell lines reveals culture-induced copy number changes and loss of heterozygosity. Nat Biotechnol 28:371–377.
13. Hussein SM, NN Batada, S Vuoristo, RW Ching, R Autio, E Närvä, S Ng, M Sourour, R Hämäläinen, et al. (2011). Copy number variation and selection during reprogramming to pluripotency. Nature 471:58–62.
14. Laurent LC, I Ulitsky, I Slavin, H Tran, A Schork, R Morey, C Lynch, JV Harness, S Lee, et al. (2011). Dynamic changes in the copy number of pluripotency and cell proliferation genes in human ESCs and iPSCs during reprogramming and time in culture. Cell Stem Cell 8:106–118.
15. Ji J, SH Ng, V Sharma, D Neculai, S Hussein, M Sam, Q Trinh, GM Church, JD Mcpherson, A Nagy and NN Batada. (2012). Elevated coding mutation rate during the reprogramming of human somatic cells into induced pluripotent stem cells. Stem Cells 30:435–440.
16. Pasi CE, A Dereli-Öz, S Negrini, M Friedli, G Fragola, A Lombardo, G Van Houwe, L Naldini, S Casola, et al. (2011). Genomic instability in induced stem cells. Cell Death Differ 18:745–753.
17. Mayshar Y, U Ben-David, N Lavon, J-C Biancotti, B Yakir, AT Clark, K Plath, WE Lowry and N Benvenisty. (2010). Identification and classification of chromosomal aberrations in human induced pluripotent stem cells. Cell Stem Cell 7:521–531.
18. Andrews PW, MM Matin, AR Bahrami, I Damjanov, P Gokhale and JS Draper. (2005). Embryonic stem (ES) cells and embryonal carcinoma (EC) cells: opposite sides of the same coin. Biochem Soc Trans 33:1526–1530.
19. Ayres FM, AD Cruz da, P Steele and BW Glickman. (2006). Low doses of gamma ionizing radiation increase hprt mutant frequencies of TK6 cells without triggering the mutator phenotype pathway. Genet Mol Biol 29:558–561.
20. Li I-C and EH Chu. (1987). Evaluation of methods for the estimation of mutation rates in cultured mammalian cell populations. Mutat Res Lett 190:281–287.
21. Green MH, JP O'Neill and J Cole. (1995). Suggestions concerning the relationship between mutant frequency and mutation rate at the hprt locus in human peripheral T-lymphocytes. Mutat Res 334:323–339.
22. Cervantes RB, JR Stringer, C Shao, JA Tischfield and PJ Stambrook. (2002). Embryonic stem cells and somatic cells differ in mutation frequency and type. Proc Natl Acad Sci U S A 99:3586–3590.
23. Tsuda H, K Sasaki and N Tanaka. (2005). Establishment of hypoxanthine phosphoribosyl-transferase (HPRT)-locus mutation assay system in mouse ES cells. Alternatives to Animal Testing and Experimentation 11:118–128.
24. Stambrook PJ, C Shao, M Stockelman, G Boivin, SJ Engle and JA Tischfield. (1996). APRT: a versatile in vivo resident reporter of local mutation and loss of heterozygosity. Environ Mol Mutagen 28:471–482.
25. Hong Y, RB Cervantes, E Tichy, JA Tischfield and PJ Stambrook. (2007). Protecting genomic integrity in somatic cells and embryonic stem cells. Mutat Res 614:48–55.
26. Adewumi O, B Aflatoonian, L Ahrlund-Richter, M Amit, PW Andrews, G Beighton, PA Bello, N Benvenisty, LS Berry, et al. (2007). Characterization of human embryonic stem cell lines by the International Stem Cell Initiative. Nat Biotechnol 25:803–816.
27. Lund RJ, E Närvä and R Lahesmaa. (2012). Genetic and epigenetic stability of human pluripotent stem cells. Nat Rev Genet 13:732–744.
28. Dvorak P, D Dvorakova, S Koskova, M Vodinska, M Najvirtova, D Krekac and A Hampl. (2005). Expression and potential role of fibroblast growth factor 2 and its receptors in human embryonic stem cells. Stem Cells 23:1200–1211.
29. Kunova M, K Matulka, L Eiselleova, A Salykin, I Kubikova, S Kyrylenko, A Hampl and P Dvorak. (2013). Adaptation to robust monolayer expansion produces human pluripotent stem cells with improved viability. Stem Cells Transl Med 2:246–254.
30. Krutá M, L Bálek, R Hejnová, Z Dobšáková, L Eiselleová, K Matulka, T Bárta, P Fojtík, J Fajkus, et al. (2013). Decrease in abundance of apurinic/apyrimidinic endonuclease causes failure of base excision repair in culture-adapted human embryonic stem cells. Stem Cells 31:693–702.
31. Gruss HJ, N Boiani, DE Williams, RJ Armitage, CA Smith and RG Goodwin. (1994). Pleiotropic effects of the CD30 ligand on CD30-expressing cells and lymphoma cell lines. Blood 83:2045–2056.
32. Bonatti S, A Di Leonardo, L Mariani, R Randazzo and G Sciandrello. (1982). Selection in HAT medium is not a reliable method for the study of reversion from 6-thioguanine resistance to sensitivity. Mutat Res 104:377–381.
33. Barta T, D Dolezalova, Z Holubcova and A Hampl. (2013). Cell cycle regulation in human embryonic stem cells: links to adaptation to cell culture. Exp Biol Med (Maywood) 238:271–275.
34. Zou G-M, M-H Luo, A Reed, MR Kelley and MC Yoder. (2007). Ape1 regulates hematopoietic differentiation of embryonic stem cells through its redox functional domain. Blood 109:1917–1922.
35. Leshchiner I, K Alexa, P Kelsey, I Adzhubei, CA Austin-Tse, JD Cooney, H Anderson, MJ King, RW Stottmann, et al. (2012). Mutation mapping and identification by whole-genome sequencing. Genome Res 22:1541–1548.
36. Hoffman LM, L Hall, JL Batten, H Young, D Pardasani, EE Baetge, J Lawrence and MK Carpenter. (2005). X-Inactivation status varies in human embryonic stem cell lines. Stem Cells 23:1468–1478.
37. Sustáčková G, S Legartová, S Kozubek, L Stixová, J Pacherník and E Bártová. (2012). Differentiation-independent fluctuation of pluripotency-related transcription factors and

other epigenetic markers in embryonic stem cell colonies. Stem Cells Dev 21:710–720.
38. Tchieu J, E Kuoy, MH Chin, H Trinh, M Patterson, SP Sherman, O Aimiuwu, A Lindgren, S Hakimian, et al. (2010). Female human iPSCs retain an inactive X chromosome. Cell Stem Cell 7:329–342.
39. Hall LL, M Byron, J Butler, KA Becker, A Nelson, M Amit, J Itskovitz-Eldor, J Stein, G Stein, C Ware and JB Lawrence. (2008). X-inactivation reveals epigenetic anomalies in most hESC but identifies sublines that initiate as expected. J Cell Physiol 216:445–452.
40. Shen Y, Y Matsuno, SD Fouse, N Rao, S Root, R Xu, M Pellegrini, AD Riggs and G Fan. (2008). X-inactivation in female human embryonic stem cells is in a nonrandom pattern and prone to epigenetic alterations. Proc Natl Acad Sci U S A 105:4709–4714.
41. Silva SS, RK Rowntree, S Mekhoubad and JT Lee. (2008). X-chromosome inactivation and epigenetic fluidity in human embryonic stem cells. Proc Natl Acad Sci U S A 105: 4820–4825.
42. Liu W, Y Yin, Y Jiang, C Kou, Y Luo, S Huang, Y Zheng, S Li, Q Li, et al. (2011). Genetic and epigenetic X-chromosome variations in a parthenogenetic human embryonic stem cell line. J Assist Reprod Genet 28:303–313.
43. Amenduni M, R De Filippis, AYL Cheung, V Disciglio, MC Epistolato, F Ariani, F Mari, MA Mencarelli, Y Hayek, et al. (2011). iPS cells to model CDKL5-related disorders. Eur J Hum Genet 19:1246–1255.
44. Ananiev G, EC Williams, H Li and Q Chang. (2011). Isogenic pairs of wild type and mutant induced pluripotent stem cell (iPSC) lines from Rett syndrome patients as in vitro disease model. PLoS One 6:e25255.
45. Pomp O, O Dreesen, DFM Leong, O Meller-Pomp, TT Tan, F Zhou and A Colman. (2011). Unexpected X chromosome skewing during culture and reprogramming of human somatic cells can be alleviated by exogenous telomerase. Cell Stem Cell 9:156–165.
46. Cheung AYL, LM Horvath, L Carrel and J Ellis. (2012). X-chromosome inactivation in rett syndrome human induced pluripotent stem cells. Front Psychiatry 3:24.
47. Mekhoubad S, C Bock, AS de Boer, E Kiskinis, A Meissner and K Eggan. (2012). Erosion of dosage compensation impacts human iPSC disease modeling. Cell Stem Cell 10: 595–609.
48. Kim D, C-H Kim, J-I Moon, Y-G Chung, M-Y Chang, B-S Han, S Ko, E Yang, KY Cha, R Lanza and K-S Kim. (2009). Generation of human induced pluripotent stem cells by direct delivery of reprogramming proteins. Cell Stem Cell 4:472–476.
49. Marchetto MCN, C Carromeu, A Acab, D Yu, GW Yeo, Y Mu, G Chen, FH Gage and AR Muotri. (2010). A model for neural development and treatment of Rett syndrome using human induced pluripotent stem cells. Cell 143:527–539.
50. Olariu V, NJ Harrison, D Coca, PJ Gokhale, D Baker, S Billings, V Kadirkamanathan and PW Andrews. (2010). Modeling the evolution of culture-adapted human embryonic stem cells. Stem Cell Res 4:50–56.
51. Tompkins JD, C Hall, VC Chen, AX Li, X Wu, D Hsu, LA Couture and AD Riggs. (2012). Epigenetic stability, adaptability, and reversibility in human embryonic stem cells. Proc Natl Acad Sci U S A 109:12544–12549.
52. Chen Y, L Guo, J Chen, X Zhao, W Zhou, C Zhang, J Wang, L Jin, D Pei and F Zhang. (2014). Genome-wide CNV analysis in mouse induced pluripotent stem cells reveals dosage effect of pluripotent factors on genome integrity. BMC Genomics 15:79.
53. Mallon BS, RS Hamilton, OA Kozhich, KR Johnson, YC Fann, MS Rao and PG Robey. (2014). Comparison of the molecular profiles of human embryonic and induced pluripotent stem cells of isogenic origin. Stem Cell Res 12: 376–386.
54. Mallon BS, JG Chenoweth, KR Johnson, RS Hamilton, PJ Tesar, AS Yavatkar, LJ Tyson, K Park, KG Chen, YC Fann and RDG McKay. (2013). StemCellDB: the human pluripotent stem cell database at the National Institutes of Health. Stem Cell Res 10:57–66.
55. Gore A, Z Li, H-L Fung, JE Young, S Agarwal, J Antosiewicz-Bourget, I Canto, A Giorgetti, MA Israel, et al. (2011). Somatic coding mutations in human induced pluripotent stem cells. Nature 471:63–67.
56. Lister R, M Pelizzola, YS Kida, RD Hawkins, JR Nery, G Hon, J Antosiewicz-Bourget, R O'Malley, R Castanon, et al. (2011). Hotspots of aberrant epigenomic reprogramming in human induced pluripotent stem cells. Nature 471: 68–73.
57. Marchetto MCN, GW Yeo, O Kainohana, M Marsala, FH Gage and AR Muotri. (2009). Transcriptional signature and memory retention of human-induced pluripotent stem cells. PLoS One 4:e7076.
58. Hussein SMI, J Elbaz and AA Nagy. (2013). Genome damage in induced pluripotent stem cells: assessing the mechanisms and their consequences. BioEssays 35:152–162.
59. Zhang M, C Yang, H Liu and Y Sun. (2013). Induced pluripotent stem cells are sensitive to DNA damage. Genomics Proteomics Bioinformatics 11:320–326.
60. Bárta T, V Vinarský, Z Holubcová, D Doležalová, J Verner, Š Pospíšilová, P Dvořák and A Hampl. (2010). Human embryonic stem cells are capable of executing G1/S checkpoint activation. Stem Cells 28:1143–1152.
61. Tichy ED, L Liang, L Deng, J Tischfield, S Schwemberger, G Babcock and PJ Stambrook. (2011). Mismatch and base excision repair proficiency in murine embryonic stem cells. DNA Repair 10:445–451.
62. Momcilović O, S Choi, S Varum, C Bakkenist, G Schatten and C Navara. (2009). Ionizing radiation induces ataxia telangiectasia mutated-dependent checkpoint signaling and G_2 but not G_1 cell cycle arrest in pluripotent human embryonic stem cells. Stem Cells 27:1822–1835.
63. Serrano L, L Liang, Y Chang, L Deng, C Maulion, S Nguyen and JA Tischfield. (2010). Homologous recombination conserves DNA sequence integrity throughout the cell cycle in embryonic stem cells. Stem Cells Dev 20:363–374.
64. Bañuelos CA, JP Banáth, SH MacPhail, J Zhao, CA Eaves, MD O'Connor, PM Lansdorp and PL Olive. (2008). Mouse but not human embryonic stem cells are deficient in rejoining of ionizing radiation-induced DNA double-strand breaks. DNA Repair 7:1471–1483.
65. Tichy ED, R Pillai, L Deng, L Liang, J Tischfield, SJ Schwemberger, GF Babcock and PJ Stambrook. (2010). Mouse embryonic stem cells, but not somatic cells, predominantly use homologous recombination to repair double-strand DNA breaks. Stem Cells Dev 19:1699–1711.
66. Adams BR, SE Golding, RR Rao and K Valerie. (2010). Dynamic dependence on ATR and ATM for double-strand break repair in human embryonic stem cells and neural descendants. PLoS One 5:e10001.

67. Luo LZ, S Gopalakrishna-Pillai, SL Nay, S-W Park, SE Bates, X Zeng, LE Iverson and TR O'Connor. (2012). DNA repair in human pluripotent stem cells is distinct from that in non-pluripotent human cells. PLoS One 7:e30541.
68. Hyka-Nouspikel N, J Desmarais, PJ Gokhale, M Jones, M Meuth, PW Andrews and T Nouspikel. (2012). Deficient DNA damage response and cell cycle checkpoints lead to accumulation of point mutations in human embryonic stem cells. Stem Cells 30:1901–1910.
69. Momcilovic O, L Knobloch, J Fornsaglio, S Varum, C Easley and G Schatten. (2010). DNA damage responses in human induced pluripotent stem cells and embryonic stem cells. PLoS One 5:e13410.
70. Ha GH, HS Kim, CG Lee, HY Park, EJ Kim, HJ Shin, JC Lee, KW Lee and CW Lee. (2008). Mitotic catastrophe is the predominant response to histone acetyltransferase depletion. Cell Death Differ 16:483–497.
71. Liao S, Y Matsumoto and H Yan. (2007). Biochemical reconstitution of abasic DNA lesion replication in *Xenopus* extracts. Nucleic Acids Res 35:5422–5429.
72. Iraqui I, Y Chekkal, N Jmari, V Pietrobon, K Fréon, A Costes and SAE Lambert. (2012). Recovery of arrested replication forks by homologous recombination is error-prone. PLoS Genet 8:e1002976.

Address correspondence to:
Vladimír Rotrekl
Department of Biology
Faculty of Medicine
Masaryk University
Kamenice 5
Brno 61265
Czech Republic

E-mail: vrotrekl@med.muni.cz

Received for publication December 16, 2013
Accepted after revision May 15, 2014
Prepublished on Liebert Instant Online XXXX XX, XXXX